Letters

Standing Wave Compensation-Based Harmonic Propagation Mitigation for Closed-Loop Distribution Feeder

Min Zhang, Xiaofeng Sun, *Member, IEEE*, Jiaxun Teng, Lei Qi, Hong Shen, and Xin Li

***Abstract*—The concepts of impedance matching and infinite feeder simulation are currently the mainstream solutions to the problem of background harmonic propagation and magnification on distribution feeders, and their principle is to eliminate reflected waves, which can dampen the harmonic voltage-magnifying factor to around 1. The standing wave compensation mitigation scheme proposed in this letter is based on a completely different concept, which can extend the feeder length to an integer multiple of the harmonic wavelength equivalently by constructing a virtual feeder. At this time, the reflection effect does not disappear but transfers to another state, and the maximum harmonic voltage-magnifying factor on the feeder is limited to 1. Furthermore, since the magnifying factor at most positions on the feeder is obviously lower than this limit, the proposed standing wave compensation-based active power filter (SWC-APF) can obtain significantly better mitigation performance than conventional schemes regardless of the installation location, and the required power capacity will not increase. Finally, the experimental results verify the effectiveness of the proposed scheme.**

***Index Terms*—Active power filter (APF), distribution feeder, harmonic propagation, standing wave compensation (SWC).**

I. Introduction

THE application of shunt capacitor banks and underground/submarine cables may lead to background harmonic propagation along distribution feeders, which will magnify the harmonic voltages seriously and deteriorate the power quality of the bus voltage [1].

Wada et al. [2] proposed the resistive active power filter (RAPF) based on voltage detection that can effectively dampen background harmonic propagation on a radial feeder, and its principle is based on the impedance matching idea in transmission line theory, which can suppress the harmonic voltage-magnifying factor on the feeder around 1. Subsequently, some optimization schemes have been proposed, and the attenuation scheme based on standing wave phase shifting can significantly improve the mitigation performance [3].

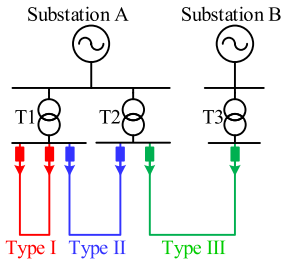

Fig. 1. Configuration of closed-loop distribution feeders.

With the demand for high power supply reliability from users, closed-loop distribution has been adopted by many utility power systems instead of open-loop distribution. For closed-loop distribution feeders, there are mainly three configurations, Type I: both sides of the feeder are connected to the same transformer, Type II: both sides of the feeder are connected to different transformers of the same substation, Type III: both sides of the feeder are connected to different substations [4], as shown in Fig. 1. This letter focuses on the closed-loop feeder of Type I, as it has better reliability and lower construction investment compared to other types [5].

The problem of background harmonic propagation also exists in closed-loop distribution feeders, and the RAPF is still effective. Based on the analysis of the distributed-parameter model, the optimal installation location should be the midpoint of the feeder [5]. According to the transmission line theory, the background harmonic propagation is caused by reflection effects, and in addition to impedance matching, reflected waves can also be eliminated on an infinite long feeder. The long-feeder simulator active power filter (LFS-APF) based on this concept has stronger adaptability [6], but the improvement of mitigation performance is limited. The optimal installation position for both RAPF and LFS-APF is the feeder midpoint, and when deviated, the mitigation performance will worsen significantly. The impedance converter scheme implemented with series and parallel APF can achieve good performance when installed at any position on the feeder [7], which is also based on the concept of infinite feeder simulation.

Manuscript received 22 May 2024; revised 1 July 2024; accepted 18 July 2024. Date of publication 23 July 2024; date of current version 11 September 2024. This work was supported in part by the Central Guidance for Local Scientific and Technological Development Funding Project under Grant 236Z2101G and in part by the Natural Science Foundation of Hebei Province under Grant E2024203170 and Grant E2021203162. *(Corresponding authors: Xiaofeng Sun and Hong Shen.)*

The authors are with the Key Laboratory of Power Electronics for Energy Conversion and Motor Drive of Hebei Province, Department of Electrical Engineering, Yanshan University, Qinhuangdao 066004, China (e-mail: zhangmin_ysu@stumail.ysu.edu.cn; sxf@ysu.edu.cn; tengjiaxun@stumail.ysu.edu.cn; qil@ysu.edu.cn; shenhong@ysu.edu.cn; yddylixin@ysu.edu.cn).

Color versions of one or more figures in this article are available at https://doi.org/10.1109/TPEL.2024.3432311.

Digital Object Identifier 10.1109/TPEL.2024.3432311

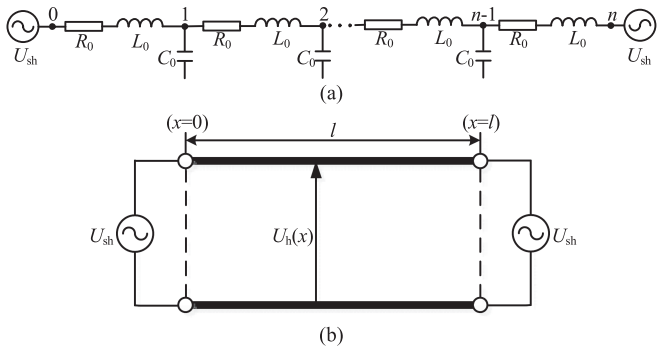

Fig. 2. Model of closed-loop distribution feeder. (a) Lumped-parameter model. (b) Distributed-parameter model.

TABLE I
PARAMETERS OF CLOSED-LOOP DISTRIBUTION FEEDER

Parameters	Value
Fundamental frequency	50 Hz
Feeder inductance L_0	2 mH/km
Feeder capacitance C_0	25 μF/km
Feeder resistance R_0	0.36 Ω/km

In order to further improve the mitigation performance, the standing wave compensation-based scheme is proposed in this letter, which is completely different from the conventional impedance matching and infinite feeder simulation concepts, the proposed scheme is not to eliminate the reflected wave, but to extend the feeder length to an integer multiple of the harmonic wavelength; equivalently, at this time, the antinode of the standing wave is exactly located at the harmonic source, then the harmonic voltage-magnifying factor at all positions on the feeder will not be greater than 1. In addition, due to the retention of the standing wave shape, the magnifying factor near the node will be very low, so the mitigation performance will be significantly improved compared with the conventional scheme.

II. Proposed Standing Wave Compensation-Based Mitigation Scheme

A. Analysis of Background Harmonic Voltage Propagation

Fig. 2(a) shows the lumped-parameter model of the closed-loop distribution feeder, the propagation and magnification of background harmonic voltage on the feeder is caused by resonance between the feeder inductance L_0 and the feeder capacitance C_0 (including power factor correction capacitance and cable parasitic capacitance). The distributed-parameter model shown in Fig. 2(b) can be used to analyze the background harmonic propagation law on the feeder [2], [3], [4], [5], [6], [7], U_{sh} is harmonic voltage source and l is feeder length.

The circuit parameters of the feeder are shown in Table I [6], and both theoretical analysis and experiments in this letter are based on this parameter.

For the distributed-parameter model of feeder, the characteristic impedance Z_{ch}, the propagation constant γ_h, and the wavelength λ_h of the hth harmonic can be expressed as

$$Z_{ch} = \sqrt{\frac{R_0 + j\omega_h L_0}{G_0 + j\omega_h C_0}} \tag{1}$$

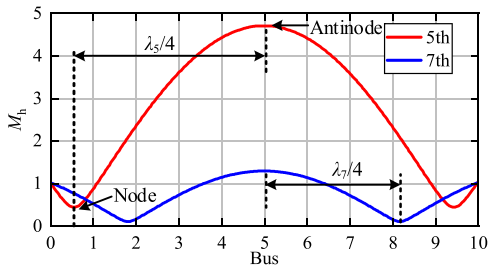

Fig. 3. Harmonic voltage standing wave on 10 km closed-loop distribution feeder.

$$\gamma_h = \sqrt{(G_0 + j\omega_h C_0)(R_0 + j\omega_h L_0)} = \alpha_h + j\beta_h \tag{2}$$

$$\lambda_h = \frac{2\pi}{\beta_h} \tag{3}$$

where α_h and β_h are attenuation constant and phase constant, respectively.

According to the theory of transmission line, the harmonic voltage standing wave on the closed-loop distribution feeder can be expressed as [5]

$$U_h(x) = \frac{\sinh[\gamma_h(l-x)]}{\sinh(\gamma_h l)} U_{sh} + \frac{\sinh(\gamma_h x)}{\sinh(\gamma_h l)} U_{sh}. \tag{4}$$

The harmonic voltage-magnifying factor on the feeder is defined as

$$M_h(x) = \left|\frac{U_h(x)}{U_{sh}}\right| = \left|\frac{\sinh[\gamma_h(l-x)] + \sinh(\gamma_h x)}{\sinh(\gamma_h l)}\right|. \tag{5}$$

Equation (5) indicates that the amplitude of harmonic voltage on the feeder changes periodically, and the period is π/β_h, which is equal to one-half of the wavelength $\lambda_h/2$. In addition, the wave peak occurs at the feeder midpoint($x = l/2$), and both ends of the feeder have unity factor because they are directly connected to the harmonic source. Taking a 10 km feeder as an example, the harmonic voltage-magnifying factor at any position on the feeder is shown in Fig. 3. The distribution state of harmonic voltages on feeders is called standing waves, which are generated by the superposition of the incident wave and the reflected wave of the harmonic voltage. The highest and lowest points of the standing wave are known as the antinode and node, respectively.

It can be seen that the magnification degree of the harmonic voltage depends on the relationship between the feeder length l and the harmonic wavelength λ_h, the closer the node of the standing wave is to the feeder ends, the more severe the harmonic propagation and amplification will be.

Based on (5), the relationship between the maximum harmonic voltage-magnifying factor and length can be drawn, as shown in Fig. 4. It can be seen that when the feeder length l is equal to an integer multiple of the harmonic wavelength λ_h, the harmonic voltage-magnifying factor at any position on the feeder cannot be greater than 1, which means that harmonic voltage will not be magnified.

If lossless feeder ($R_0 = 0$) is considered, the maximum harmonic voltage-magnifying factor on the feeder is approximately

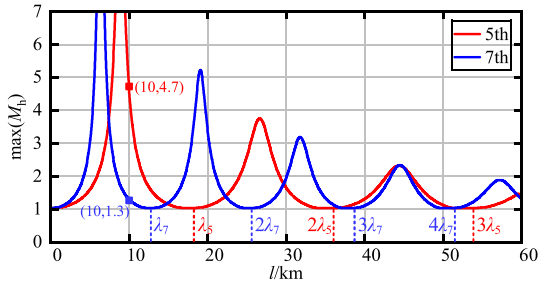

Fig. 4. Relationship curve between feeder length and maximum harmonic voltage magnifying-factor.

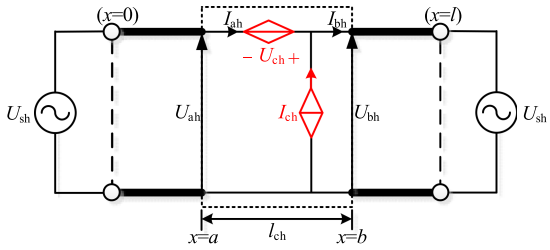

Fig. 5. Schematic diagram of standing wave compensation.

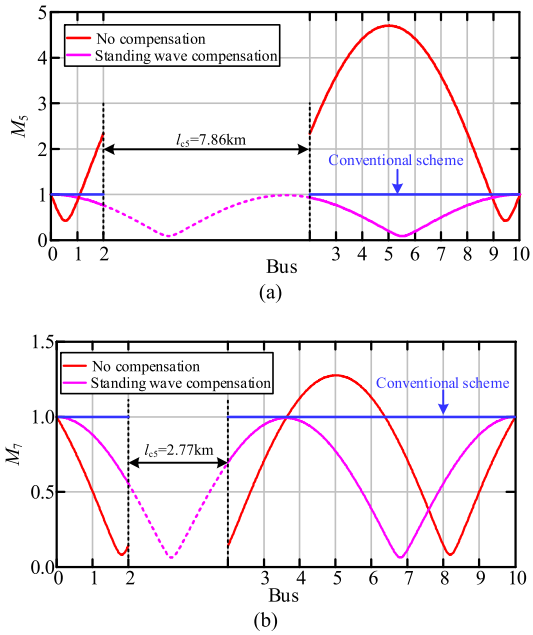

Fig. 6. Harmonic voltage standing wave on 10 km closed-loop distribution feeder before and after standing wave compensation. (a) Fifth harmonic. (b) Seventh harmonic.

$$\max[M_{\rm h}(x)] \approx \frac{1}{|\cos(\pi l/\lambda_{\rm h})|}. \tag{6}$$

Equation (6) also indicates that harmonic propagation on feeder with integer multiples of wavelengths is the weakest.

B. Principle of Standing Wave Compensation

Equivalent extension of feeder length to integer multiples of the harmonic wavelength is the essence of standing wave compensation, but in practical systems, the actual length of the feeder cannot be changed. However, a certain length of feeder can be simulated by controlled source, and the schematic diagram is shown in Fig. 5. Since the feeder has two ports, it needs to be equivalent by combining a series voltage source $U_{\rm ch}$ with a parallel current source $I_{\rm ch}$, and $l_{\rm ch}$ is the extended length of the feeder and also the compensation length of the standing wave, a is compensation position.

According to Fig. 5, the voltage and current at $x = a$ and $x = b$ satisfy the following relationship [8]:

$$\begin{cases} U_{\rm bh} = U_{\rm ah}\cosh(\gamma_{\rm h} l_{\rm ch}) - Z_{\rm ch} I_{\rm ah}\sinh(\gamma_{\rm h} l_{\rm ch}) \\ I_{\rm bh} = I_{\rm ah}\cosh(\gamma_{\rm h} l_{\rm ch}) - \frac{U_{\rm ah}}{Z_{\rm ch}}\sinh(\gamma_{\rm h} l_{\rm ch}) \end{cases}. \tag{7}$$

Equation (7) can be transformed into

$$\begin{cases} U_{\rm ch} = U_{\rm bh} - U_{\rm ah} = U_{\rm ah}[\cosh(\gamma_{\rm h} l_{\rm ch}) - 1] \\ -Z_{\rm ch} I_{\rm ah}\sinh(\gamma_{\rm h} l_{\rm ch}) \\ = U_{\rm ah} \cdot k_{\rm vh1} e^{j\theta_{\rm vh1}} + I_{\rm ah} \cdot k_{\rm ih1} e^{j\theta_{\rm ih1}} \\ I_{\rm ch} = I_{\rm bh} - I_{\rm ah} = I_{\rm ah}[\cosh(\gamma_{\rm h} l_{\rm ch}) - 1] - \frac{U_{\rm ah}}{Z_{\rm ch}}\sinh(\gamma_{\rm h} l_{\rm ch}) \\ = U_{\rm ah} \cdot k_{\rm vh2} e^{j\theta_{\rm vh2}} + I_{\rm ah} \cdot k_{\rm ih2} e^{j\theta_{\rm ih2}} \end{cases}. \tag{8}$$

Equation (8) is the expression of the controlled voltage and current source, it indicates that a certain length of feeder simulation can be implemented by sampling $U_{\rm ah}$ and $I_{\rm ah}$, and according to Fig. 4, the optimal compensation length is

$$l_{\rm ch} = k\lambda_{\rm h} - l(k = 0, 1, 2, 3\cdots). \tag{9}$$

The harmonic voltage standing wave before and after compensation is shown in Fig. 6, and the compensation position is Bus 2 (a = 2km). It clearly shows the effectiveness of the proposed scheme for harmonic suppression, and due to retaining the characteristics of standing waves, the magnifying factor of some buses will be very low, which is not available in existing schemes. It is worth noting that the dashed line represents the standing wave compensated by the controlled source, which does not exist in practice.

C. Control Block Diagram of SWC-APF

The proposed standing wave compensation scheme is implemented by the standing wave compensation-based active power filter (SWC-APF), and in view of Fig. 5 and (8), the control block diagram of SWC-APF is shown in Fig. 7. Due to the standing wave compensation length of each harmonic being different, selective harmonic extraction is used and implemented by synchronous reference frame transformation, which also achieves control of harmonic phase angle [9].

III. Evaluation of Mitigation Performance

When the harmonic voltage is magnified on the feeder, it is reasonable to judge the severity of harmonic propagation by the maximum magnifying factor in Fig. 4, and the larger the maximum factor, the more severe the propagation. However, for the evaluation of mitigation performance, both existing and proposed schemes can effectively mitigate harmonic propagation and prevent harmonic magnification, but customers and

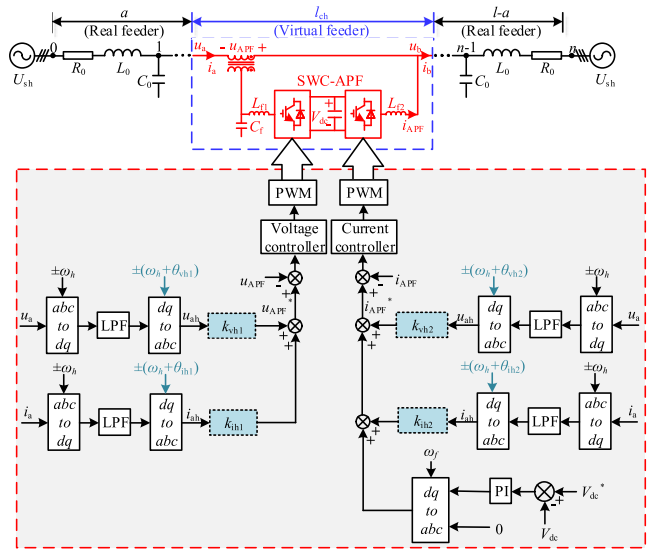

Fig. 7. Control block diagram of SWC-APF.

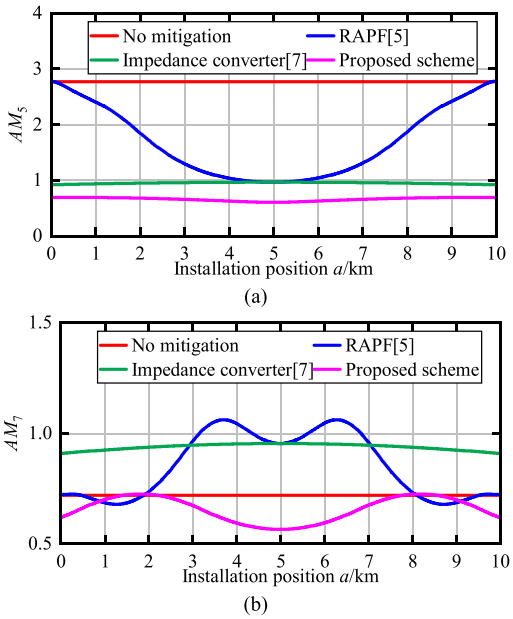

Fig. 8. Mitigation performance comparison of different schemes. (a) Fifth harmonic. (b) Seventh harmonic.

electricity suppliers always hope that the total harmonic distortion (THD) of bus voltage is as low as possible. Therefore, to quantify the voltage harmonic level on the whole feeder, the average value of the harmonic voltage-magnifying factor (*AM*) on the feeder is used [3], [10], the smaller the *AM*, the better the mitigation performance. For proposed scheme, it is expressed as

$$AM_{\mathrm{h}} = \frac{1}{l}\left(\int_0^a M_{\mathrm{h}}(x)dx + \int_{a+l_{\mathrm{ch}}}^{l+l_{\mathrm{ch}}} M_{\mathrm{h}}(x)dx\right). \tag{10}$$

In order to illustrate the robustness of the standing wave compensation scheme to the change of installation position, and the superiority of the mitigation performance compared with the existing schemes. The *AM* of different schemes as the installation (compensation) position changes is drawn and shown in Fig. 8. It can be seen that the proposed scheme can consistently maintain better performance even when the installation position changes.

IV. Experimental Verification

In order to verify the correctness of the above theoretical analysis and the effectiveness of the proposed standing wave compensation mitigation scheme, a down-scaled single-phase closed-loop distribution feeder with SWC-APF experimental platform was built, the photograph is shown in Fig. 9, and the system parameters are shown in Table II.

The experimental results of the RAPF [5], impedance converter [7], and SWC-APF installed on bus 2 are shown in Fig. 10, it can be seen that the proposed scheme can obtain better mitigation performance than the state-of-the-art impedance converter scheme, and the rms values of APF voltage u_{APF} and current i_{APF} of both are basically the same, which indicates that the SWC-APF does not consume more power capacity.

The harmonic voltage-magnifying factor experimental results under different compensation positions are shown in Fig. 11, which illustrates that the mitigation performance of the proposed

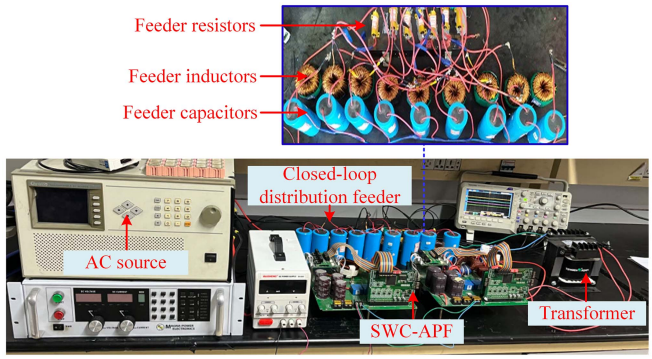

Fig. 9. Photograph of the experimental platform.

TABLE II
Parameters of Experimental Platform

	Parameters	Value
Source	Grid simulator	Chroma6530
	Fundamental frequency f_0	50 Hz
	Background harmonic	5th:3% 7th:2%
Feeder	Length l	10 km
	Resistance of per-unit length R_0	0.36 Ω ±5%
	Inductance of per-unit length L_0	2 mH ±5%
	Capacitance of per-unit length C_0	25 μF±5%
APF	Transformer ratio	1:1
	Switching frequency f_s	10 kHz
	Switching device	IKW20N60T
	Controller	TMS320F28335

scheme is always optimal compared to other schemes, regardless of the installation location. Moreover, the experimental results of Fig. 11(a) are consistent with the harmonic voltage standing wave after compensation in Fig. 6, which also verifies the correctness of the theoretical analysis.

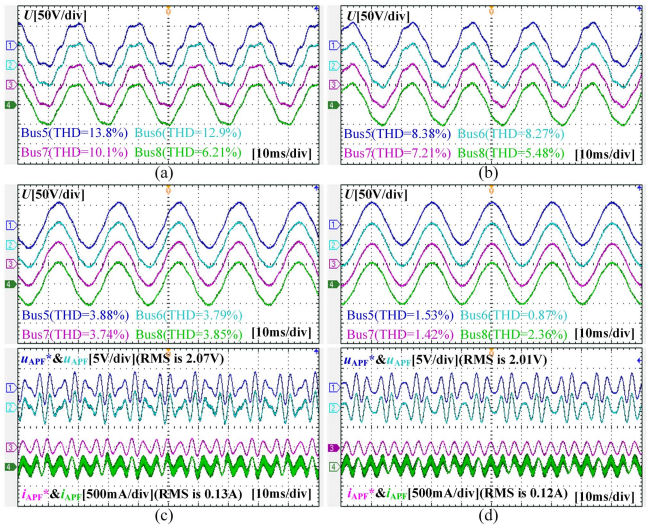

Fig. 10. Experimental waveforms of bus voltage and APF. (a) No mitigation. (b) RAPF scheme. (c) Impedance converter scheme. (d) Proposed scheme.

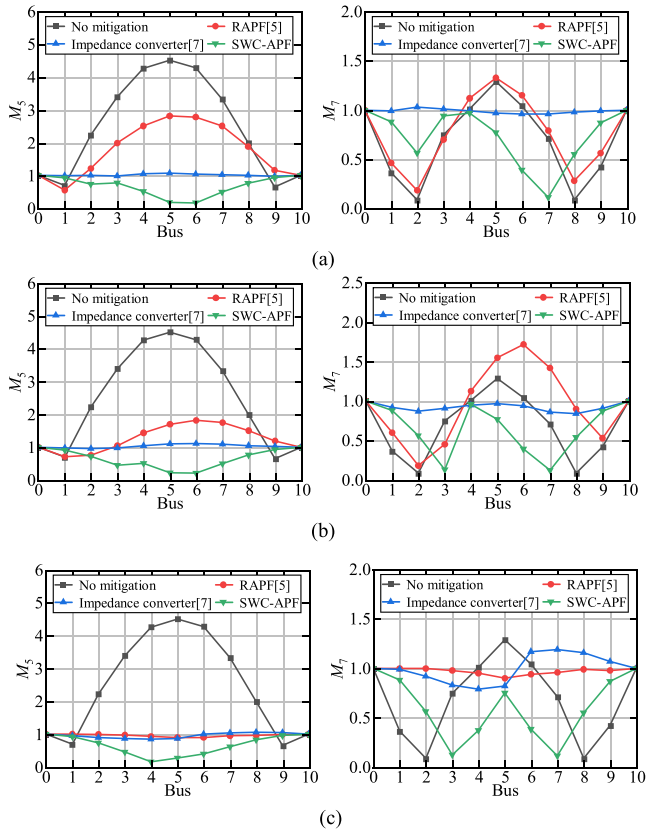

Fig. 11. Experimental results under different compensation positions. (a) Installed on bus 2. (b) Installed on bus 3. (c) Installed on bus 5.

V. Discussions

A. Comparison With Existing Methods

In order to demonstrate the superiority of the proposed scheme, a detailed comparison was made with existing methods, as shown in Table III. There are three mainstream methods

TABLE III
Comparison of Previous Works

Ref	Concept	Hardware configuration	Mitigation performance	Robustness to installation position changes
[5]	Impedance matching	Parallel APF	Medium	Poor
[6]	Infinite feeder simulation	Parallel APF	Medium	Poor
[7]	Infinite feeder simulation	Series and parallel APF	Medium	Good
Proposed scheme	Standing wave compensation	Series and parallel APF	Good	Good

to mitigate harmonic propagation on closed-loop distribution feeders, the principle of RAPF [5] is based on the concept of impedance matching, and the principle of LFS-APF [6] and impedance converter [7] is based on the concept of infinite feeder simulation.

The desired installation location for the RAPF and LFS-APF is to be connected in parallel at the midpoint of the feeder, as the mitigation performance will be significantly worse if deviated. The impedance converter has added a series APF compared to the previous two, but it is robust to changes in installation position, that is, it can maintain expected mitigation performance regardless of where it is installed on the feeder.

For the SWC-APF proposed in this letter, its hardware configuration is the same as the impedance converter, but the principle is completely different. The existing methods aim to eliminate the reflected wave on the feeder, however, the proposed scheme transfers the reflection effect to another state, in which the maximum magnifying factor on the feeder is clamped to 1. In addition, the magnifying factor at most positions on the feeder is significantly lower than 1 due to the retention of the standing wave feature. Therefore, the proposed scheme can achieve better mitigation performance and only involve the improvement of control.

B. Technical and Economic Feasibility

For the technical implementation of the proposed scheme, although standing wave compensation is a completely new concept for harmonic mitigation, the specific implementation is not complicated, and the control algorithm is also quite mature. This is benefited by the flourishing development of active filtering technology, including selective harmonic extraction [11], harmonic voltage and current closed-loop control [12], and other aspects.

In terms of economy, the proposed SWC-APF needs to be achieved through the coordination of series and parallel converters, which indeed requires a certain amount of investment and increases the cost of distribution network construction. Fortunately, in modern distribution networks, delta-type uninterruptible power supply (UPS) [13], unified power flow controller (UPFC) [14], and energy router (ER) [15] all have the same topology structure with SWC-APF, which means that the hardware equipment is readily available and the proposed scheme can be embedded as an additional function. Therefore, the cost of the proposed scheme is only software upgrade.

VI. Conclusion

Based on the idea of extending the feeder length equivalently by constructing a virtual feeder, this letter proposes a background harmonic propagation mitigation scheme based on standing wave compensation, which can limit the harmonic voltage-magnifying factor on the feeder to less than 1, and the factor near the node on the feeder will be significantly less than 1 due to the retention of the characteristics of the standing wave. Therefore, compared to the conventional scheme that can only dampen the factor to around 1, the proposed scheme has a better suppression effect and the power capacity will not increase.

References

[1] J. He, Y. W. Li, R. Wang, and C. Zhang, "Analysis and mitigation of resonance propagation in grid-connected and islanding microgrids," *IEEE Trans. Energy Convers.*, vol. 30, no. 1, pp. 70–81, Mar. 2015.

[2] K. Wada, H. Fujita, and H. Akagi, "Consideration of a shunt active filter based on voltage detection for installation on a long distribution feeder," *IEEE Trans. Ind. Appl.*, vol. 38, no. 4, pp. 1123–1130, Jul./Aug. 2002.

[3] M. Zhang et al., "Research on the standing wave phase shifting based background harmonic voltages attenuation," *IEEE Trans. Power Electron.*, vol. 37, no. 3, pp. 3434–3450, Mar. 2022.

[4] T.-H. Chen, W.-T. Hung, J.-C. Gu, G.-C. Pu, Y.-F. Hsu, and T.-Y. Guo, "Feasibility study of upgrading primary feeders from radial and open-loop to normally closed-loop arrangement," *IEEE Trans. Power Syst.*, vol. 19, no. 3, pp. 1308–1316, Aug. 2004.

[5] T. L. Lee and S. H. Hu, "Discrete frequency-tuning active filter to suppress harmonic resonances of closed-loop distribution power systems," *IEEE Trans. Power Electron.*, vol. 26, no. 1, pp. 137–148, Jan. 2011.

[6] X. Sun et al., "Study of a novel equivalent model and a long-feeder simulator-based active power filter in a closed-loop distribution feeder," *IEEE Trans. Ind. Electron.*, vol. 63, no. 5, pp. 2702–2712, May 2016.

[7] X. Sun, L. Yang, R. Wang, R. Han, H. Shen, and Z. Chen, "A novel impedance converter for harmonic damping in loop power distribution systems," *IEEE J. Emerg. Sel. Topics Power Electron.*, vol. 4, no. 1, pp. 162–173, Mar. 2016.

[8] R. Ludwig and P. Bretchko, *RF Circuit Design: Theory and Applications*. Englewood Cliffs, NJ, USA: Prentice-Hall, 2000, pp. 159–161.

[9] Z. Wang et al., "Adaptive harmonic impedance reshaping control strategy based on a consensus algorithm for harmonic sharing and power quality improvement in microgrids with complex feeder networks," *IEEE Trans. Smart Grid*, vol. 13, no. 1, pp. 47–57, Jan. 2022.

[10] H. Zhai et al., "An optimal compensation method of shunt active power filters for system-wide voltage quality improvement," *IEEE Trans. Ind. Electron.*, vol. 67, no. 2, pp. 1270–1281, Feb. 2020.

[11] H. Liu, H. Hu, H. Chen, L. Zhang, and Y. Xing, "Fast and flexible selective harmonic extraction methods based on the generalized discrete Fourier transform," *IEEE Trans. Power Electron.*, vol. 33, no. 4, pp. 3484–3496, Apr. 2018.

[12] P. Santiprapan, K. Areerak, and K. Areerak, "An adaptive gain of proportional-resonant controller for an active power filter," *IEEE Trans. Power Electron.*, vol. 39, no. 1, pp. 1433–1446, Jan. 2024.

[13] A. Nasiri, "Digital control of three-phase series-parallel uninterruptible power supply systems," *IEEE Trans. Power Electron.*, vol. 22, no. 4, pp. 1116–1127, Jul. 2007.

[14] R. A. Modesto, S. A. O. Da Silva, A. A. De Oliveira, and V. D. Bacon, "A versatile unified power quality conditioner applied to three-phase four-wire distribution systems using a dual control strategy," *IEEE Trans. Power Electron.*, vol. 31, no. 8, pp. 5503–5514, Aug. 2016.

[15] X. Zhao, P. Bai, X. Wang, C. Zhang, X. Guo, and Q. Zhao, "Coupling constraint behavior and design method for two-degree-of-freedom in series-parallel architecture electric energy router," *IEEE Trans. Smart Grid*, vol. 15, no. 2, pp. 1680–1693, Mar. 2024.